

C2

MECHANISMS OF MATERIAL REMOVAL IN THE
SOLID PARTICLE EROSION OF DUCTILE MATERIALS

Ronald A. Mayville
(M. S. thesis)

RECEIVED
LAWRENCE
BERKELEY LABORATORY

JUL 10 1978

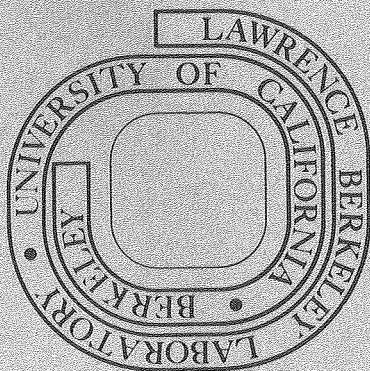
June 1978

LIBRARY AND
DOCUMENTS SECTION

Prepared for the U. S. Department of Energy
under Contract W-7405-ENG-48

TWO-WEEK LOAN COPY

*This is a Library Circulating Copy
which may be borrowed for two weeks.
For a personal retention copy, call
Tech. Info. Division, Ext. 6782*



C2

— LEGAL NOTICE —

This report was prepared as an account of work sponsored by the United States Government. Neither the United States nor the Department of Energy, nor any of their employees, nor any of their contractors, subcontractors, or their employees, makes any warranty, express or implied, or assumes any legal liability or responsibility for the accuracy, completeness or usefulness of any information, apparatus, product or process disclosed, or represents that its use would not infringe privately owned rights.

MECHANISMS OF MATERIAL REMOVAL IN THE SOLID PARTICLE
EROSION OF DUCTILE MATERIALS

Masters of Science Ronald A. Mayville Mechanical Engineering

ABSTRACT

The behavior of materials subject to erosion has been studied extensively in the last 20 years, yet little is known about the physical mechanisms of material removal. This work is an attempt to determine the mechanisms by which material is removed from a ductile metal surface when subjected to the impingement of a stream of angular abrasive particles. The particular case considered is one where the stream impinges at angles that are nearly normal to the average surface. In this case, material appears to be removed in the form of platelets that result when a protrusion from the average surface is severely plastically deformed (as if being spread over the surface) by the impingement of a smooth side of a particle.

CONTENTS

Introduction	1
Experimental Conditions	2
General Erosion Behavior	4
Terminology	4
Factors Influencing Erosion	7
Mechanisms of Material Removal	11
Mechanisms at Low Angles of Impingement	12
Material Displaced and Efficiency	14
Mechanisms of Material Removal for High-Angle Impingement	17
A Detailed Observation of the Erosion Process	18
Experiments	18
Results and Analysis	22
Conclusions and Recommendations	32
Acknowledgments	35
References	36

INTRODUCTION

Solid particle erosion is a type of wear most often considered detrimental, but may be used to advantage. The handling of particulate matter is a problem in coal conversion processes, while sandblasting requires an erosive agent. Because of the many erosion problems that arise in industry, and the potential applications of erosion, there has been an active interest in both developing our knowledge of erosion in general and in examining the mechanisms of material removal associated with erosion.

The importance of understanding the physical mechanisms of material removal is clear. It would aid greatly in the design of new materials to combat erosive wear and allow the engineer to predict the life of a component from an analytic model based on the mechanisms. Although a great deal of knowledge on erosion behavior exists, little accurate information on physical mechanisms is available. Hence, there is a lack of analytic models. This is due to the complex nature of the process, and many investigators attempt to idealize conditions in an erosion experiment to diminish the vast number of variables. Common idealizations in solid particle erosion experiments include the use of ideal ductile and brittle surface materials and particles of regular geometry, such as spherical steel shot.

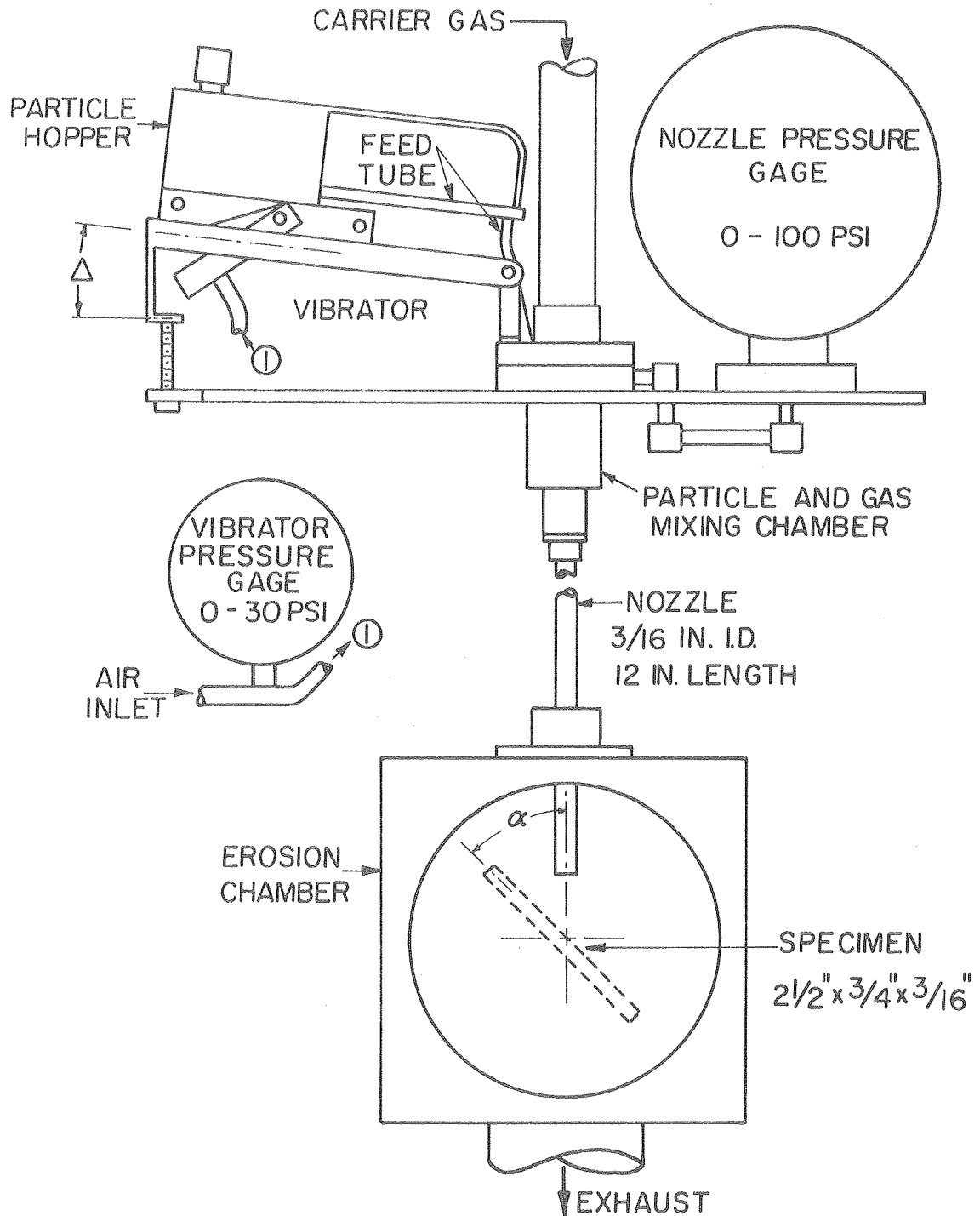
This approach has led to the viewpoint that a microcutting process occurs as the mechanism of material removal for grazing angles of impingement, but the mechanism controlling material removal at high angles of impingement is not known. Because of this, I attempt here to observe the mechanism of material removal for high angles of impingement.

EXPERIMENTAL CONDITIONS

The tester used for the erosion experiments in this work is described in detail in Ref. 1, but a brief description is given here for completeness.

The abrasive particles are fed into an air stream at room temperature by a vibrating hopper. The frequency of vibration and inclination of the hopper determine the particle feed rate. The rate of flow of the air, which determines the velocity of the particles in the stream, is easily controllable. A schematic diagram of the tester is given in Fig. 1. Passing through a 5 mm i.d. nozzle, the abrasive stream impinges upon a sample which may be inclined at any angle to the direction of flow by rotating the holder in which it is placed. Velocity measurements are made by using an apparatus² that consists of two parallel plates separated by a fixed distance, and rotating at the same constant angular velocity. The plane of the plates is perpendicular to the direction of particle flow. Some particles pass through a radial slit in the top plate so that they impinge at a point angularly displaced from the slot position on the bottom plate. The location of this point is dependent on the velocity of the particles, the angular velocity of the plates, and the distance between the plates. In this work, velocities of 31 and 62 m/sec are used and are estimated to be accurate within 10%.

An attempt was made to simulate conditions encountered in a coal gasifier by eroding commercially pure aluminum (1100-0) with angular SiC particles. This choice was based on the following considerations:



XBL775-5525

Fig. 1. A schematic diagram of the Sheldon Erosion Tester (SET).

1. Aluminum is a soft, ductile, f.c.c. metal and at room temperature should simulate the strength and hardness of the harder, ductile, f.c.c. metals normally used to combat erosion at elevated temperatures in coal gasifiers, (e.g., 310 stainless steel).
2. Some of the particles encountered in the coal gasification process, such as the shale particles contained in char, are similar to SiC particles in shape and sometimes in hardness.
3. The ductility and single phase of aluminum and the angular prismatic shape and strength of SiC allow for simplifying assumptions in analysis.

In a later section of this work, detailed observations of the mechanism of material removal for normal angles of impingement are attempted. An AMR scanning electron microscope along with an EDAX x-ray analyzer are used for this purpose. Little preparation is required for the direct observation of the eroded surface, but for cross sections it is necessary to cut the specimen with a Buehler Isomet Diamond Saw and to mount the specimen in a special Bakelite mixture developed to preserve the edge.

GENERAL EROSION BEHAVIOR

Terminology

When speaking of erosion by an abrasive stream, discussion will be confined to an abrasive stream that consists of solid particles and some fluid. The particles are considered as the erosive agent, and the fluid is considered to do little damage. This latter assumption is valid if the fluid is a gas. On the other hand, a liquid impinging on a surface may produce cavitation erosion. Gas as a carrier

fluid also minimizes the effect of flow over a surface on the trajectories of a particle, except for very small particles.

The loading rate is a measure of the density of the abrasive particles in the fluid stream. It is often defined as the amount of abrasive in a unit mass or volume of the fluid. A somewhat more meaningful definition is the amount of abrasive impinging on a unit area of surface per unit time. This definition facilitates design when the volume removed for each unit of abrasive impinged is known.

Conventional terminology for the geometry of impingement of a single particle is illustrated in Fig. 2. The particle impinges at an angle to the average plane of the surface with a velocity U_0 . Some workers have shown that the orientation with which the particle impinges is of importance,³ but this is difficult to describe because of the irregular geometry of most particles. When spherical steel shot particles are used, orientation is of no consequence.

When plotting the curve of mass loss of an eroded ductile metal vs the amount of abrasive particles impinged upon it, a very reproducible phenomenon occurs (Fig. 3). After an amount of abrasive has been impinged, the amount depending on a number of parameters, the slope of the curve becomes essentially constant. This slope is defined as the erosion rate E_R for the particular material under the conditions of erosion. The erosion rate is the common parameter used to measure the resistance of a material to erosion, and may be expressed in units of g/g, the mass of material removed per unit mass of abrasive impinged, or cm^3/g , the volume of material removed per unit mass of abrasive impinged.

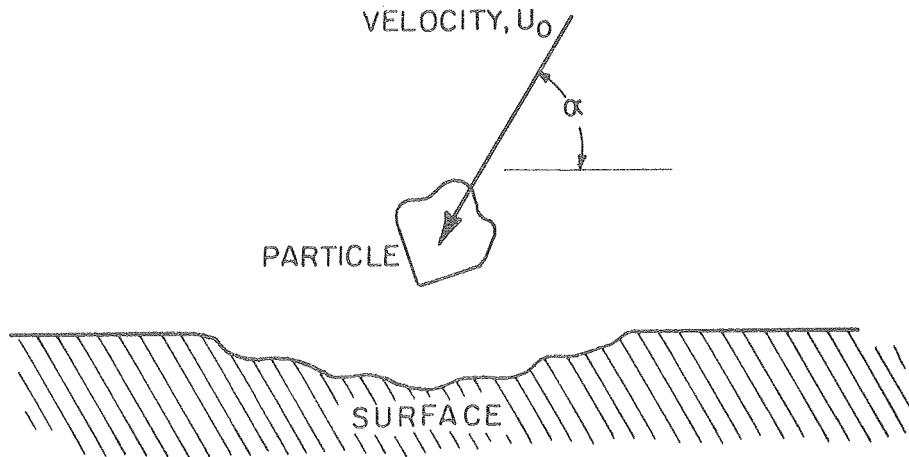
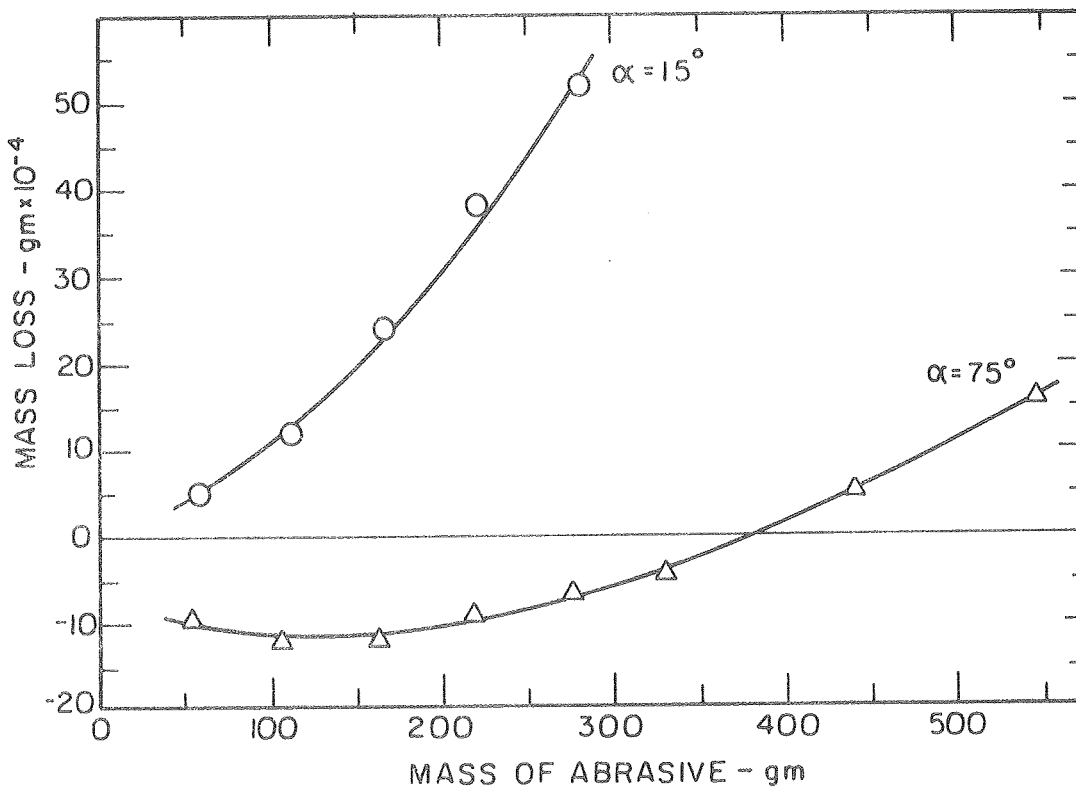


Fig. 2. Geometry of impingement of a single abrasive particle.



XBL 7711-6465

Fig. 3. Mass loss vs mass of abrasive impinged for Al 1100-0 eroded with $250 \mu\text{m}$ diameter SiC particles at a velocity of 31 m/sec.

The period before the mass loss vs mass of abrasive curve becomes constant is known as the incubation period. The duration of this period depends on many factors, including the properties of the surface material, angle of impingement, and velocity of the eroding particles. The period is generally short for low angles of impingement but is much longer for the conditions of Fig. 3 where $\alpha = 75^\circ$. An accurate explanation for this effect has yet to be given.

When eroding ductile and brittle materials, such as aluminum and glass, two very different types of behavior occur as illustrated by considering the E_R vs α curves for the two materials (Fig. 4a). These curves represent nearly ideal ductile and brittle behavior under erosive conditions. Most materials exhibit some intermediate behavior. An interesting point is that some brittle materials behave in a ductile manner when eroded by very small particles.⁴

Factors Influencing Erosion

There are a multitude of factors that influence erosion behavior. The influence of parameters associated with the abrasive stream and the surface material on erosion rate is of particular interest.

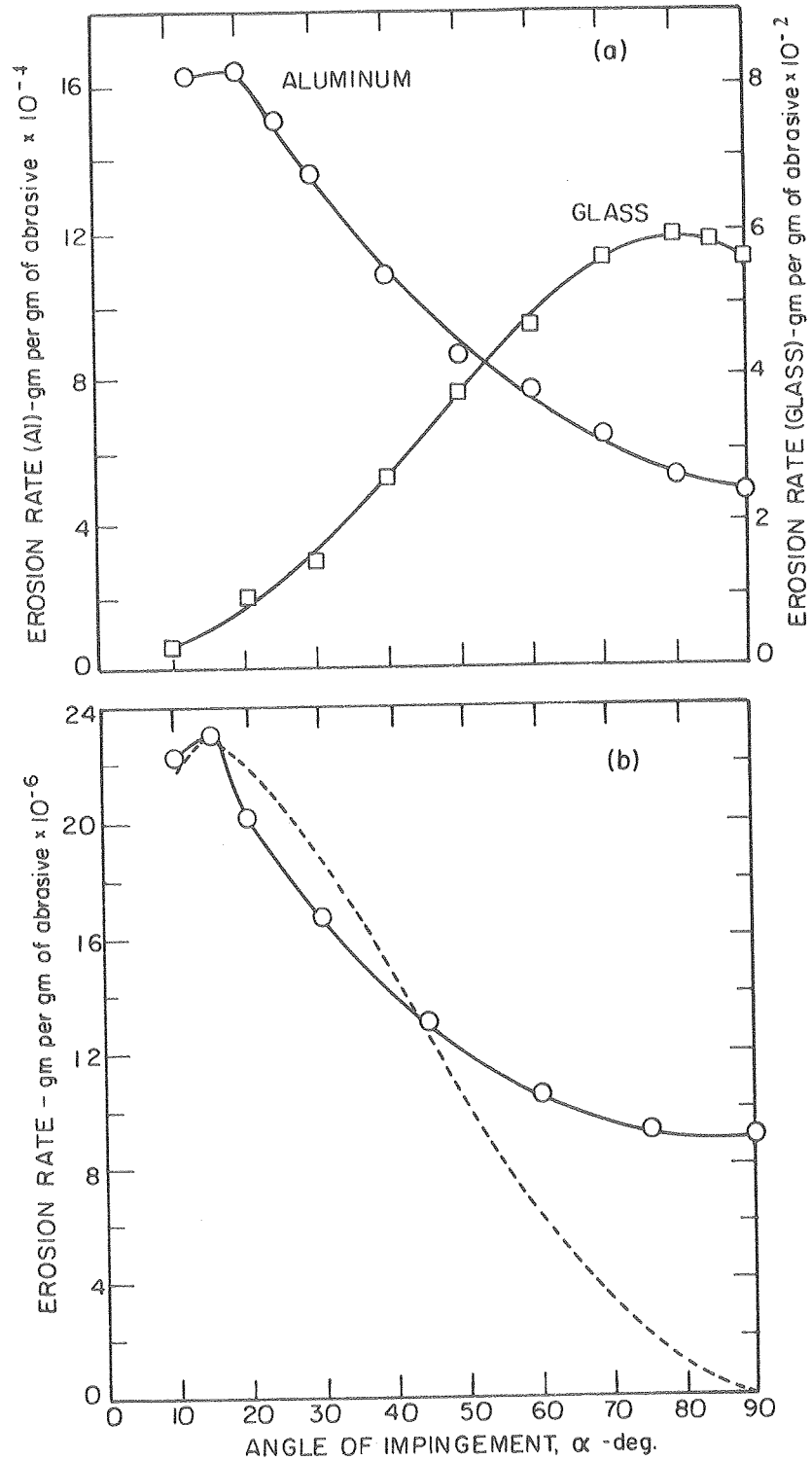
If the carrier fluid in the abrasive stream is a gas, only the particles and their density in the stream are of concern. Angular particles such as SiC or Al_2O_3 are observed to be more erosive than spherical particles such as steel spherical shot.⁵ The hardness and strength of particles have an effect on erosion rate; harder particles have been found to be more erosive,⁶ while it has been suggested that fracture of particles upon impact contributes to erosion.⁷

Of interest is the effect of particle size on erosion. There is little variation in erosion rate for particles with diameters larger than 100 μm , for all angles of impingement.^{4,7} For smaller particles, erosion rate decreases until erosion becomes negligible at a certain size, depending on test conditions. This effect may be due to the surface material approaching its ideal strength as the particle indentations become very small.

When the density of the particles in the gaseous stream, or loading rate is varied, little variation in erosion rate occurs. The tendency is for erosion to decrease as the loading rate increases, which may possibly be explained by an increasing interference of rebounding particles with impinging particles.

The relationship between erosion rate and angle of impingement for SiC particles impinging at 31m/sec on commercially pure aluminum is shown in Fig. 4b. For ductile metals the erosion rate is typically a maximum around $\alpha = 15^\circ$. For higher angles of impingement the erosion rate decreases continuously to a value at $\alpha = 90^\circ$ from 30 - 40% of the maximum. For the conditions of Fig. 4b the erosion rate at $\alpha = 90^\circ$ is about 40% of the maximum.

There is also a strong dependence of erosion rate on the velocity of the particles U_0 , in the abrasive stream. The literature indicates that this dependency varies between a quadratic dependence and a cubic dependence for ductile metals. There also appears to be an increase in the velocity exponent with increasing α . Table 1 lists comparisons



XBL7711-6466

Fig. 4. Erosion rate vs angle of impingement. (a) Aluminum and glass, eroded with 125 μm diameter SiC particles at a velocity of 155 m/sec (from Ref. 3). (b) Aluminum eroded with 250 μm diameter SiC particles at a velocity of 31 m/sec. Solid line--experiment; dashed line--prediction (refer to Mechanisms at Low Angles of Impingement).

Table 1. Comparison of erosion rate and velocity for commercially pure aluminum eroded with 250 μm diameter SiC particles.

α	Erosion rate - E_R g/g $\times 10^{-6}$		$n(E_R \sim U_O^n)$
	31 m/sec	62 m/sec	
15 $^\circ$	23	142	2.62
90 $^\circ$	9	66	2.87

of erosion rate vs two velocities for aluminum eroded with SiC particles at angles of impingement of 15 $^\circ$ and 90 $^\circ$. The data indicate that when a relationship of the form.

$$E_R \sim U_O^n$$

is assumed, the exponent on velocity is $n = 2.62$ for $\alpha = 15^\circ$ and $n = 2.87$ for $\alpha = 90^\circ$.

The surface properties of the material being eroded have a large effect on erosion rate as is demonstrated by considering the difference between erosion rate for ductile and brittle materials. For ductile metals, the hardness has been used as an indication of a material's ability to resist erosion. Hardness is also used in analyses to represent the flow stress of the material, which is assumed to deform plastically. The question of whether to use some work-hardened surface hardness rather than the annealed surface hardness is based on the idea that strain hardening of the surface occurs as steady-state erosion is approached. This is supported by the fact that cold work has little effect on erosion rate. But it is possible that high temperatures at the surface associated with high strain rates caused by the impinging particles may cancel the effect of work hardening. Correlation between

annealed surface hardness and erosion rate for low angles of impingement indicate an inverse relationship.⁸

Prompted by the observation that some materials with nearly identical hardnesses have different erosion rates, other surface properties and combinations of surface properties have been used for correlations with erosion rate.^{6,9} The effect of microstructure on erosion rate is studied in Ref. 10. It is observed that different phases in the Al-Cu system with the same hardnesses have erosion rates that differ by as much as 30%.

MECHANISMS OF MATERIAL REMOVAL

Knowledge of the mechanisms of material removal controlling the erosion process is necessary for a clear understanding and prediction of erosion phenomena. The mechanism by which material is removed at grazing angles of impingement for ductile metals is generally accepted as being similar to a microcutting process. That is, a particle impinges on the surface, cutting a chip from it or at least raising material well above the average surface.

No such simple mechanism has been observed to control the material removal process at high angles of impingement. Although many mechanisms have been proposed for this case (see below), the problem remains unresolved. Resolving the problem has been the main driving force to the present work, for which the review of general erosion behavior presented above and the outline of an existing analysis presented below is most helpful.

Mechanisms at Low Angles of Impingement

By using the idea of a microcutting process,¹¹ one worker was able to do a dynamic analysis of a single particle impinging on a ductile metal surface and arrive at various predictions for erosion behavior. It is useful to cover the general assumptions of Ref. 11, separate from specific assumptions for grazing angles, since these general assumptions are expected to be valid for high-angle impingement. These general assumptions are listed as follows:

1. The particles are angular, having very sharp corners and are of sufficient strength not to fracture.
2. The material of the surface being eroded behaves as an ideal plastic material.
3. Each particle does an equal amount of damage.

The validity of the above assumptions is supported by observations of photographs of the eroded surface to be presented later. These photographs indicate that angular indentations, relatively little fracture debris and widespread plastic deformation are quite dominant.

A generalization of assumption 3 may be more accurate. Instead of each particle doing equal damage, one can consider a cycle, or string of n particles as doing equal damage. This implies that the cycle of particles constitutes a process for which each particle may play a different part. Note that assumption 3 is a special case with $n = 1$.

The more restrictive assumptions made in the Ref. 11 analysis for grazing angles of impingement are that:

4. The material displaced is equal to the material removed.
5. There is no initial rotation of the particles prior to impingement (in effect an average condition).
6. A constant ratio of vertical to horizontal force on the particle exists (guided by grinding tests).

The ensuing dynamic analysis, assuming the resultant force of the deforming material acts at the tip of the particle, resulted in the expression for volume removal as,

$$V = \frac{mU_0^2}{4p(1+mr^2)} f(\alpha); f(\alpha) = \begin{cases} \frac{2}{P} (\sin 2\alpha - \frac{2}{P} \sin^2\alpha), & \alpha \leq \alpha_0 \\ \cos^2\alpha, & \alpha > \alpha_0 \end{cases}$$

where m = mass of a single particle,

U_0 = impingement velocity,

p = horizontal component of flow pressure between surface and particle taken as the Vicker's hardness, H_V ,

r = radius of particle,

I = moment of inertia of the particle about its mass center,

α = angle of impingement,

$P = K/(1+mr^2/I)$,

K = ratio of vertical force to horizontal force (constant).

The two expressions for $f(\alpha)$ correspond to the particle escaping from the surface and imbedding in the surface, respectively. The angle α_0 is the angle at which the transition occurs.

This analysis, which was derived under the assumption that the resultant force acts at the tip of the particle, has recently been

modified so that the resultant force acts at a distance from the tip equal to the crater depth.¹²

The analysis agrees quite well with general erosion behavior for α up to 40° , as shown in Fig. 4b. The predicted curve has been normalized so that the peak erosion values coincide. The analysis also predicts the angle of maximum erosion very well and with the modification predicts exponents on velocity of 2.2-2.5, which have been observed by many workers.

However, the analysis has its shortcomings. As indicated for the need of normalization above, predictions differ from observations quantitatively. For the case of Fig. 4b, the analysis overestimates the observed maximum erosion by a factor of 25. This factor seems to decrease with increasing velocity and is about 7 for a velocity of 155 m/sec under the same conditions as in Fig. 4b. This indicates that the assumptions are more realistic at higher velocities.

Another deficiency of the analysis, which is inherent in the proposed microcutting mechanism of material removal, is the absence of material removal predicted at near-normal impingement angles.

Material Displaced and Efficiency

In this discussion consider efficiency to be related to the number of particles required to remove a unit of material. As mentioned above, one of the assumptions made in the analysis for low-angle impingement is that the volume displaced is equivalent to the volume removed.

Consider the prediction of the analysis for commercially pure aluminum eroded with SiC particles larger than 100 μm diameter,

impinging at a velocity of 31 m/sec. Based on the moment of inertia for a sphere and cube, an approximation of I for the angular particles is $mr^2/3$. Thus for $\alpha = 15^\circ$, the expression for erosion rate (V/m) becomes approximately

$$E_R = \frac{U_0^2}{16p}$$

The annealed hardness for the aluminum is $H_V = 26.5 \text{ kg/mm}^2$, so that an estimate for the flow pressure is $p = (26.5)(9.81) = 260 \text{ MN/m}^2$.

The predicted erosion rate is thus

$$E_R = \frac{(31)^2}{16(260)} \times 10^{-3} = 2.31 \times 10^{-4} \text{ cm}^3/\text{g}.$$

The experimental value for this case obtained from Fig. 4b and divided by the density of aluminum, 2.7 g/cm^3 , is $E_R = 8.52 \times 10^{-6} \text{ cm}^3/\text{g}$.

Thus, the predicted value overestimates the observed value by about a factor of 25. This factor seems to decrease as the velocity increases; for a velocity of 15 m/sec it is about 7.

As possible explanations for the quantitative deviance of the analysis in Ref. 11, two factors are considered: the number of particles impinging ideally is a small percentage of the total, or the actual flow pressure of the surface increases markedly due to erosion. Evidence exists for both explanations.^{9,13}

Consider next the volume of material displaced by an angular particle impinging normally on a surface with flow pressure p , at a velocity U_0 . If one models the particle as a prism with triangular

type cross section at the tip of the particle, or as a conical indenter, use of Newton's second law and the assumption of axisymmetric impingement result in the same expression for volume displaced. A somewhat simpler analysis may be based on energy concepts. Thus,

$$p(V) = \frac{1}{2} mU_0^2, \quad \text{or} \quad V = \frac{mU_0^2}{2p}.$$

If the assumption is then made that the volume displaced is equal to the volume removed,

$$E_R = \frac{U_0^2}{2p}.$$

Using the same conditions as for the comparison at $\alpha = 15^\circ$,

$$E_R = \frac{(31)^2}{2(260)} \times 10^{-3} = 1.85 \times 10^{-3} \text{ cm}^3/\text{g}.$$

The observed value is $E_R = 3.33 \times 10^{-6} \text{ cm}^3/\text{g}$. In this case, the predicted value overestimates the observed value by a factor of 550.

Because no combination of the factors cited to explain the quantitative disagreement for low angle impingement can account for the disagreement here, one can conclude that the hypothesis of volume displaced = volume removed is not applicable for high-angle impingement. This conclusion is supported when one observes single-particle impingement craters in which the original surface is often visible on the bottom.¹

This last line of reasoning implies that a cycle of particles may be required to remove a unit of material, or that the unit of material removed by a single particle is very small in comparison

to the volume displaced.

Mechanisms of Material Removal For High-Angle Impingement

The inability to describe how material is removed at high angles of impingement has prompted many investigators to postulate what the mechanism might be. Some of the possibly relevant proposed mechanisms found in the literature are given below.

It has been proposed¹⁴ that a severe work hardening of the surface occurs due to the normal component of force of the impinging particles and that brittle behavior follows causing the surface to spall. On the other hand, Ref. 7 attempts to explain material removal at high angles of impingement by considering the particle to fracture so that the radially spreading fragments remove material as in low-angle impingement. In Ref. 15, the high strain rates caused by the impinging particles are considered to be of importance. These high strain rates are supposed to cause large local increases in temperature, allowing for easy flow of the material which might splatter or snag onto the particle as it rebounds from the surface. The delamination theory of wear proposed in Ref. 16 for abrasive type wear may have applicability to solid particle erosion. The theory states that stresses below the surface, caused by normal and tangential loads applied at the surface, may reach sufficient magnitude to initiate and propagate cracks there. Detailed studies in Refs. 17 and 18 support an extrusion of material from under the impinging particle as a mechanism of material removal. They^{17,18} observed that for single-particle impingements, the extruded material, or lip, tore from the surface at a critical velocity. The last mechanism considered in this review is quite

general in nature. In Ref. 8 it is mentioned that material may be removed by a low-cycle fatigue-type process for high angles of impingement. That is, a unit of material on the eroded surface is repeatedly deformed or strained by successively impinging particles until it fatigues, tearing from the surface.

Some evidence exists for all of the proposed mechanisms, and it is quite reasonable to expect that a combination of them might be occurring. Based on observations of the eroded surface given in the next section, it is doubtful that the first three mechanisms - brittle fracture, erosion by fragments, and melting - occur for the conditions of the experiments done in this investigation.

A Detailed Observation of the Erosion Process

Experiments

Probably the best way to discover what actually occurs in the solid particle erosion process, or how material is removed, would be to take a motion picture and play it back in slow motion. This would be quite difficult of course and would probably require the design of a special apparatus, but it is not the only way in which one can gain information about the progression of material displacement and removal.

By viewing a specific spot on the eroded surface before and after it has been eroded, one may observe the changes in geometry due to the impinging particles. This basic idea is used in an experiment designed to gain information on the mechanism of material removal for near-normal angles of impingement.

For this experiment, commercially pure aluminum is eroded at

an angle of $\alpha = 90^\circ$ (normal impingement) with 600 μm diameter SiC particles impinging at a velocity of 62 m/sec. The normal angle of impingement is assumed to be representative of high angles of impingement, since the erosion rate vs angle of impingement curve levels off at the high angles (Fig. 4b). This indicates that the mechanism of material removal does not vary there. Most investigators believe that there is a transition from one mechanism of material removal at low angles of impingement, cutting, to a different mechanism at high angles. This is supported in part by the rapid decline of erosion rate for angles of impingement greater than 20° - 30° often observed in experiments. The larger size particles and velocity used in this experiment result in greater deformation so that observation is made easier. This should be of little consequence in the determination of the mechanism of material removal, since the particle sizes used in this work cause little variation in erosion rate.

Specimens used for this experiment are first pre-eroded well into the region of steady-state erosion. Relocation of a specific spot on the eroded surface after successive short periods of erosion is possible by making small punch marks in the center of the eroded area. The specimen with the punch marks and a sample of the particles used to erode it, are shown in Fig. 5. Making punch marks will obviously alter the stress - strain distribution around the area of interest, but this alteration should occur mainly underneath the punch marks, having little effect on the surface between the marks.

Having identified a specific spot on the eroded surface, the area around it is photographed with the Scanning Electron Microscope;

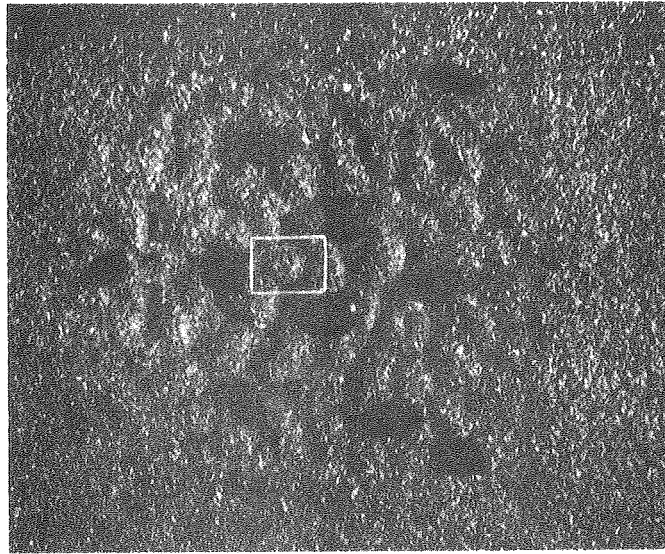


Fig. 5. The punch marks and a sample of the 600 μm diameter SiC particles on the specimen used in the progression experiment. (The square is that region shown in Fig. 7).

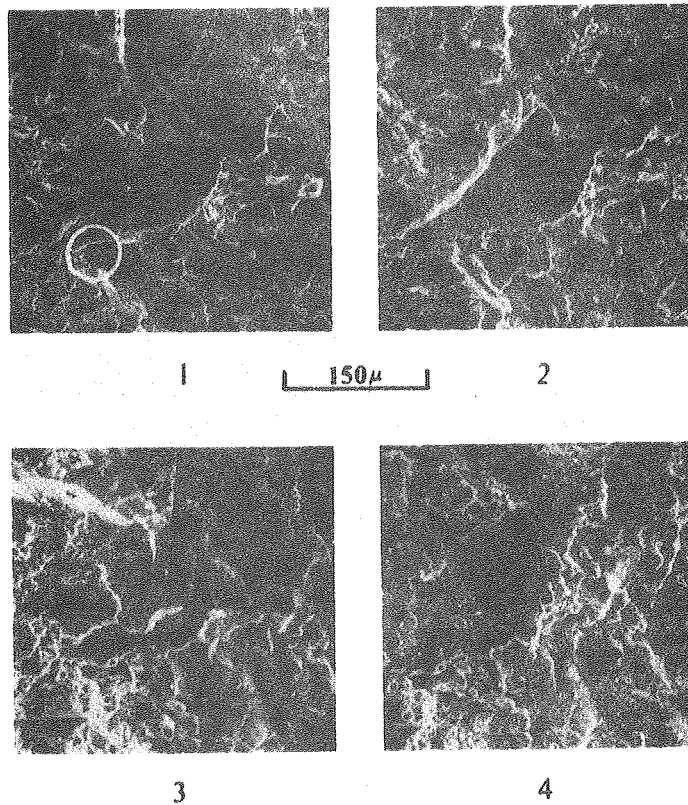


Fig. 6. Photographs of the same spot, each after successive short periods of erosion with 600 μm diameter SiC particles at $\alpha = 90^\circ$, $U_0 = 62$ m/sec. (The circle marks a spot common to all four photographs.)

in this case an area of 800 μm by 1600 μm at a magnification of 150X is mapped. These conditions allow a fairly large area to be observed in adequate detail and more activity may be investigated when a larger area is observed. After photographing the area the specimen is removed from the microscope and eroded under the same conditions with very few particles, approximately 500 to 1000. The specimen is then rephotographed at the same area, which is identifiable by the punch marks. The process is repeated several times so that by viewing the sequence of photographs, one may observe how material is successively displaced on the eroded surface (e.g., Fig. 6, to be discussed in detail below).

For additional information, other observations are made. The eroded surface is photographed at greater magnifications and at various angles inclined to the surface so that a greater appreciation of the actual geometry of deformation is possible without the use of stereo pairs.

In addition to the use of the SEM for the direct observation of the eroded surface, cross sections of specimens eroded under identical conditions are made and wear debris from the eroded surface is collected.

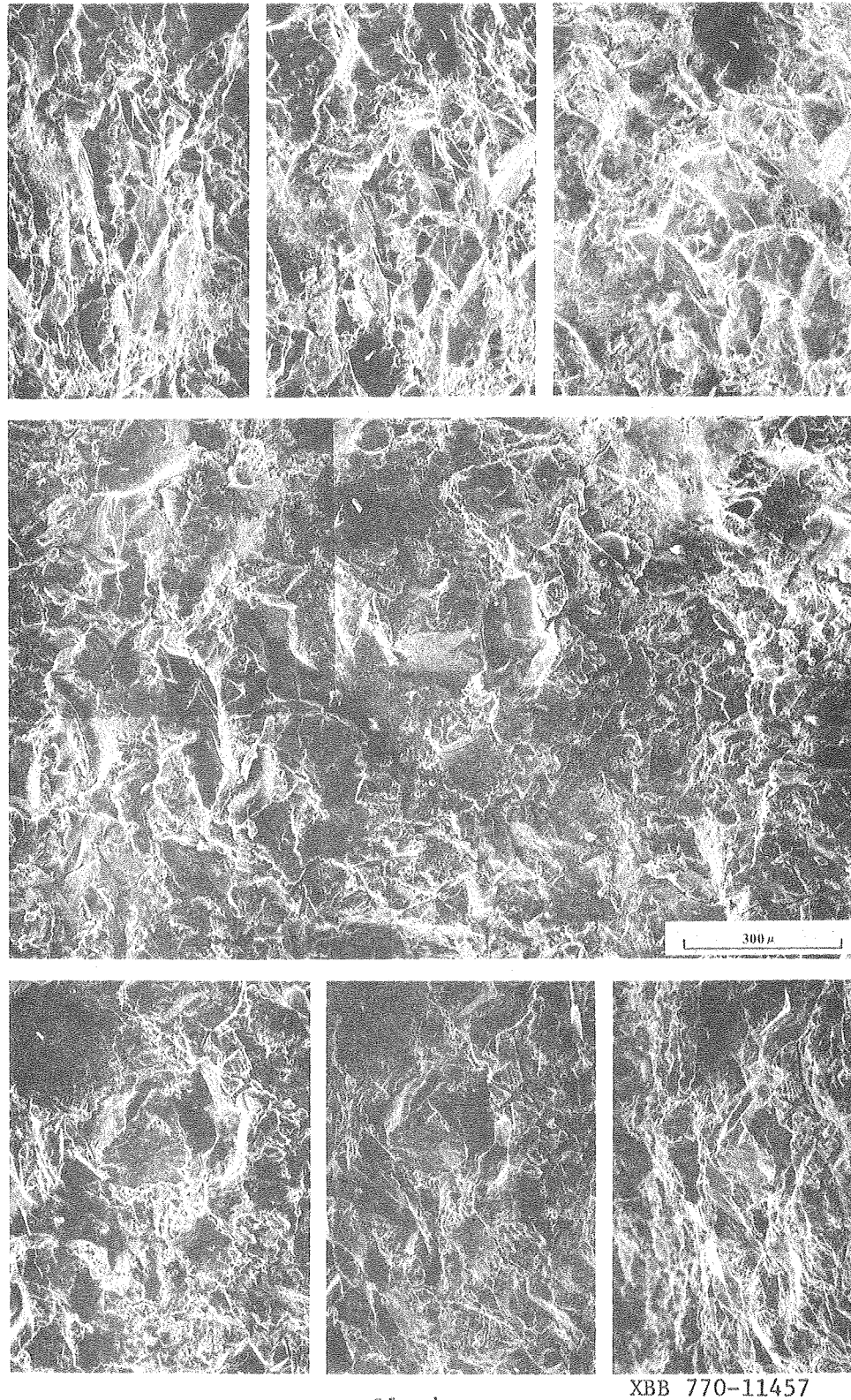
The cross sections are prepared by first cross sectioning the specimen with a Buehler Isomet diamond saw. The cross-sectioned specimen is then mounted in a special Bakelite mixture, which has excellent flow and strength properties for high edge retention. The mounted specimen is polished to a grade of 0.05 μm , being sure to never use SiC for polishing so that any SiC observed in the cross sections must be due to the impinging particles.

In order to obtain wear debris from a specimen, the erosion tester

must be thoroughly cleaned to diminish the presence of foreign matter. A simple bowl-type container is placed under the specimen in the tester so that most of the abrasive particles collect there after impingement. The collected wear debris, after being sifted through a number 200 mesh size screen (spacing-75 μm) to eliminate most of the abrasive particles, is also observed with the SEM. In Ref. 19 copper was eroded and the removed material was quite easily observed with an optical microscope. This same process is used here by eroding copper under the same conditions as the aluminum, observing the wear debris with a Zeiss Metallograph.

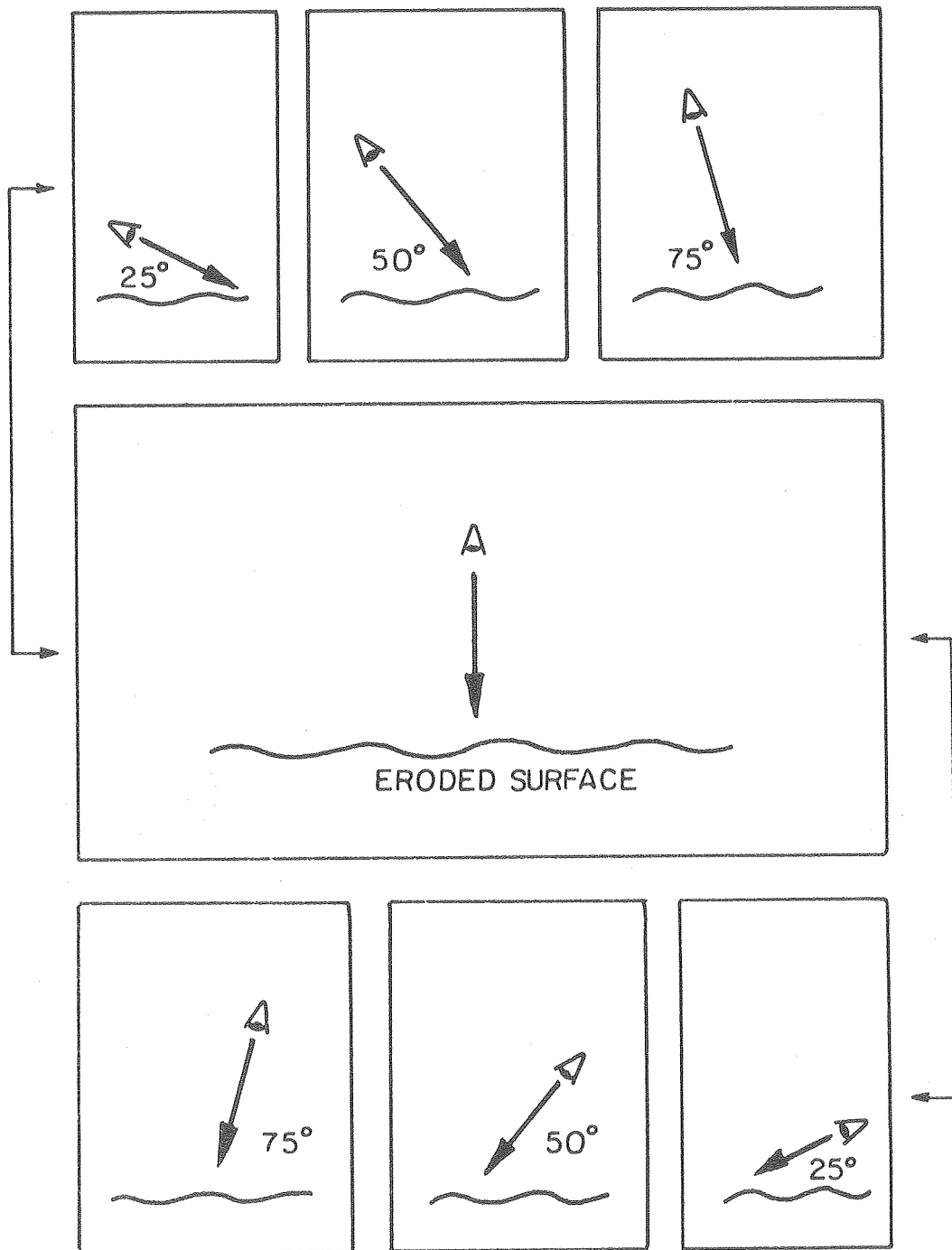
Results and Analysis

The results of these experiments proved to be instructive. Figure 7 shows the area observed in this experiment. The edges of the punch marks are barely visible on the top and bottom of the center photograph. This photograph was taken looking directly down on the surface, which is the path of the impinging particles, and indicates that a great deal of the surface has been met by the flat smooth side of a particle. The horizontal appearance of these flat areas, however, is misleading. By using the top and bottom series of photographs, which are explained in Fig. 8 and taken at angles of 25° , 50° and 75° from the average surface, one can see that the flat areas are instead often inclined at large angles to the average surface. This indicates that some particles do indeed impinge as angular indenters. But this is not always the case. Very rough areas are visible which are probably a result of the rough side of a particle impinging or the fragmentation of impinging particles. One can also see the rough pit and mound



Aluminum
XBB 770-11457

Fig. 7. The area on the specimen observed in the progression experiment, 600 μm diameter SiC particles, $\alpha = 90^\circ$, $U_0 = 62$ m/sec. Center photograph: looking directly on the specimen; top and bottom series correspond to elevation photographs. (See Fig. 8 for detailed explanation).



XBL 7711-6467

Fig. 8. An explanation of the use of Fig. 7. The eyes indicate how one is looking at the surface of a particular photograph.

character of the surface corresponding to Fig. 5. This phenomenon is characteristic of the very soft, ductile metals such as aluminum and lead, and manifests itself in the form of ripples for low angles of impingement.

Figure 6 shows four photographs of the same spot on the eroded surface after successive short periods of erosion. The first photograph (1) shows an area of the surface that is located on the slope of a mound. In the next photograph (2) there appears to have been an angular particle indentation depressing the material in the lower right-hand corner of the photograph with respect to the material in the upper left-hand corner. This edge-depression type geometry can be found all over the surface of the eroded specimen. In the third photograph (3) the material in the upper left-hand corner appears to have been smashed and spread, or sheared over the depressed material. The fourth (4) photograph shows that further spreading has occurred, but it is difficult to say whether material has been removed in the process.

This depression-smashing-spreading process is observed on a number of spots in the total area observed in this progression experiment, but in no case could it clearly be concluded that material had been removed in the process. Nevertheless, it seems reasonable to consider that material is removed in this manner, which may be roughly likened to an extrusion process. The impinging particles deform the surface in such a way that many protrusions above the average surface are created. If the flat side of a particle impinges on a protrusion, two events may occur: the protrusion may be depressed into the base

material or, if the material below the protrusion is harder or constrained to deform for some reason, the protrusion should spread, or extrude over the surface under the particles. This harder subsurface could be due to prior deformation that caused some work hardening.

If this spreading is occurring, one can expect to see layered material at points on the surface. Figure 9 illustrates a layer on the surface; the photograph is taken at an acute angle from the surface. Figure 10 shows a part of a cross section of an aluminum specimen eroded under the same conditions as for the progression experiment. It also illustrates a layer that appears to be separated from the eroded surface, but is probably connected at some point behind the plane of the photograph.

An interesting point, which is illustrated in Figure 10, is the embedment of abrasive particles in the eroded surface. That these particles are SiC is verified by use of the EDAX x-ray analyzer associated with the SEM. This phenomenon is observed across the entire cross section of the eroded surface, and the depth of embedment varies irregularly within the eroded region diminishing as one leaves the eroded region. It is possible, using Newton's second law of motion and some assumptions about particle geometry, to obtain an estimate of the depth of indentation of an angular particle. This depth, when computed for the conditions used for the progression experiments, indicates that a particle could indent to the depths at which embedded abrasive particles are observed. It is then possible that the stresses within a particle upon impingement may reach sufficient magnitude to shatter the particle, leaving a "pocket" of fragments. Indeed,

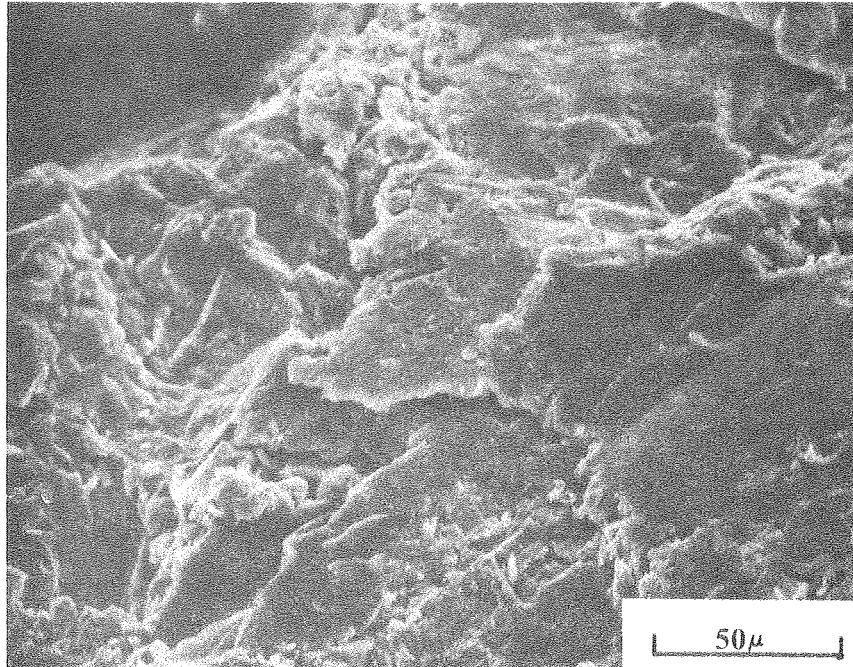
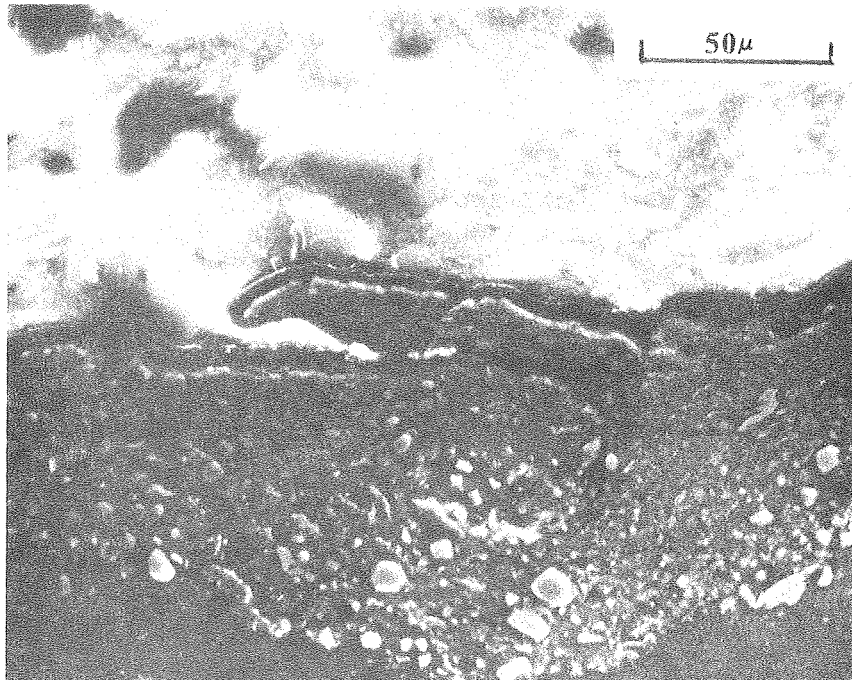


Fig. 9. A layer observed on a specimen eroded at $\alpha = 90^\circ$ with 600 μm diameter SiC particles, $U_0 = 62$ m/sec.



XBB 770-11459

Fig. 10. A cross section of a layer on a specimen eroded at 90° , with 600 μm diameter SiC particles, $U_0 = 62$ m/sec.

in the cross sections of eroded copper, a harder material than aluminum, several isolated pockets of abrasive material were observed across the entire eroded region. Since these embedded particles appear to be quite widespread it is difficult to ignore the contribution they might make to the erosion process. Depending on the distribution of the particles within the surface, it is possible that they may act as a hardening agent, aiding the process of spreading protrusions. Alternatively, the particles could act as sites for the nucleation and propagation of cracks below the surface.

Returning to the spreading phenomenon as a possible mechanism of material removal, one should ask how material is finally removed. Separation of the layers from the surface could occur in two ways:

- (1) The layer, being separated from the surface except at say one edge, might be cut from the surface by the sharp edge of an impinging particle.
- (2) The spreading, or shearing of material may cause separation of the layer from the surface by tensile strains in the direction of spreading. The tensile strains required for separation in this case would necessarily be greater than the strains at failure in a tensile test because of the compressive state of stress on the layer. The tensile strains in the layer would also be expected to increase as the component of velocity in the tangential direction increased. The tangential velocity of the abrasive particle would tend to shear the layer in addition to the spreading that occurs as a result of the normal component of velocity. As the angle of impingement decreases from $\alpha = 90^\circ$, the tangential velocity increases, but the normal component of velocity decreases, decreasing the shear force

on the particle so that there is an interaction between the two effects. Figure 12 illustrates an aluminum specimen eroded with 600 μm diameter SiC particles at a velocity of 62 m/sec at an impingement angle of 15° . The layer in the center of the photograph has been extensively sheared, or strained indicating the effect spoken of above.

In either case of material removal, one expects that the separated layers will be of platelet form. A piece of aluminum, removed by erosion from a specimen subject to the same conditions as for the progression experiments, is shown in Fig. 11. This wear particle with its flat, platelet form and jagged edges is characteristic of most of the wear particles observed for both aluminum and copper.

It is worth noting that the average facial area of the platelets is approximately 25% of the area of indentation of a particle impinging ideally. If the platelet is very thin, then its volume represents a small fraction of the volume displaced by an angular particle. Consideration of the platelet as a unit of material removed by a single particle, as opposed to the volume displaced by a single particle as the unit of material removed, results in a much higher efficiency for normal angles of impingement than that computed previously. For example, suppose the volume of a platelet is $1/25$ of the volume theoretically displaced by an angular particle. Referring to the section on material displaced and efficiency the efficiency of one particle to remove a unit of material then becomes

$$550/25 = 22.$$

This is the same order of magnitude as the efficiency computed for low angles of impingement and may thus be considered reasonable (c.f.

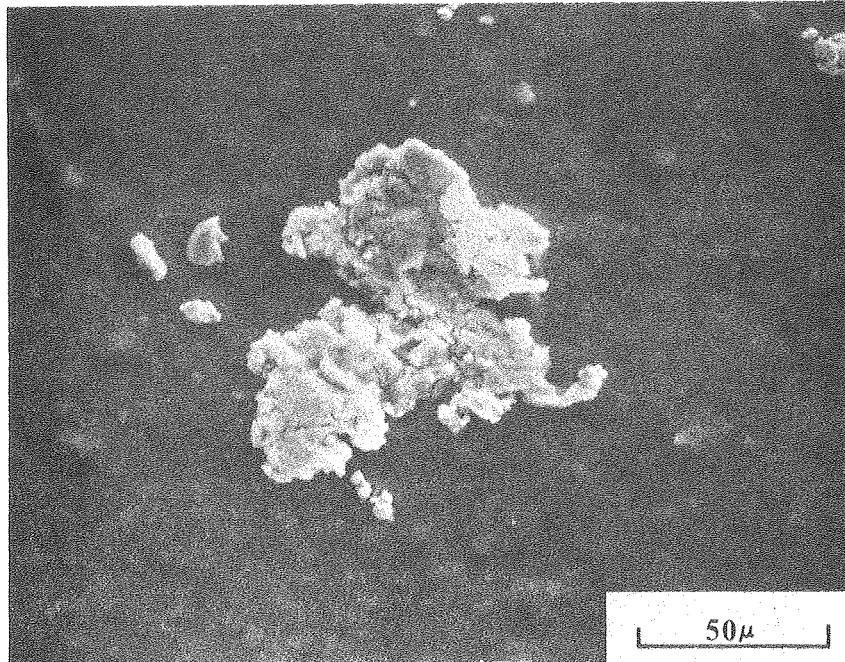
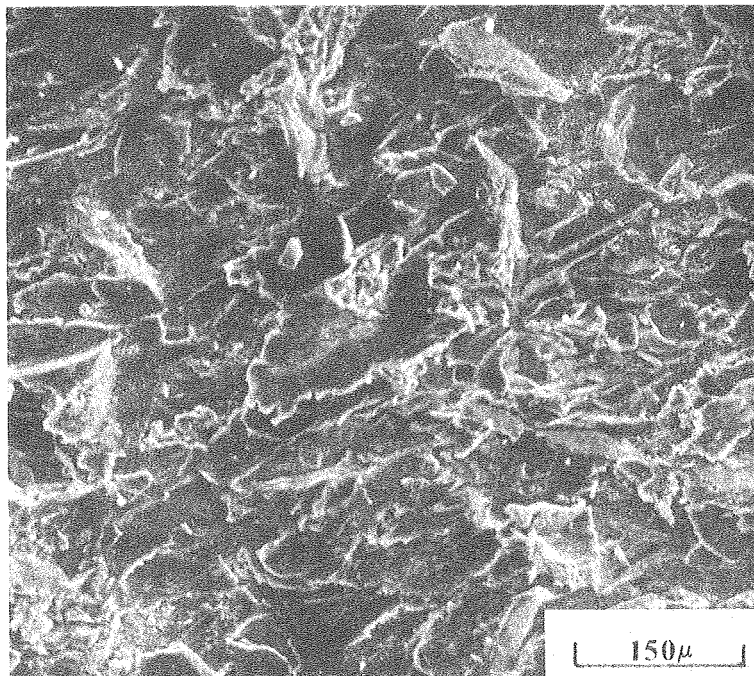


Fig. 11. A piece of aluminum removed by erosion from an aluminum specimen eroded at $\alpha = 90^\circ$ with 600 μm diameter SiC particles, $U_0 = 62/\text{sec}$.



XBB 770-11460

Fig. 12. An extensively sheared layer on an aluminum specimen eroded at $\alpha = 15^\circ$ with 600 μm diameter SiC particles, $U_0 = 62 \text{ m/sec}$.

Ref. 19). In this case, as in the case of grazing angles of impingement a cycle of particles may be required to remove a unit of material. For example, if 22 particles are required to remove a platelet, all of the material removed would be accounted for in this analysis. On the other hand, because of the relative size difference between a platelet and a particle indentation, the particle could conceivably do the work of both preparing a platelet for removal while at the same time providing the energy to remove a platelet.

CONCLUSIONS AND RECOMMENDATIONS

Solid particle erosion is indeed a complex process, and is by no means completely understood. In fact, the complexity of the process has prohibited almost everyone from providing an accurate analytic model to predict behavior. Only in the case of grazing angles of impingement has anyone had success. And even in that case, with a knowledge of the mechanism of material removal, the analysis has some important shortcomings. Nevertheless, understanding of the phenomenological aspects of erosion has progressed steadily, and the contribution of the analysis made has generalizations for the entire range of impingement angles.

For high angles of impingement the mechanism of material removal is not known. The mechanism for these high angles is generally accepted as being different from the cutting mechanism controlling low-angle impingement erosion. By observing an eroded surface before and after successive short periods of erosion, it appears that material is displaced by the spreading of protrusions on the surface by impinging particles. The process of spreading is most efficient when a flat smooth side of a particle impinges on a protrusion that has material under it which is less likely to deform. This harder material may be caused by the embedment of particles or just a gradient of work hardening. This spreading of material results in layers, or platelets of material separated from the body of the surface but connected at some edge. These platelets may then be removed by a disruption of the surface at the point of connection or by spreading to a great enough extent so that failure occurs under the tensile strains, both under the force

of impinging particles. If the platelet is considered as a unit of material, observations indicate that only a few particle impingements are necessary to remove it in order to account for the erosion rates observed at these high angles of impingement.

The spreading, or extrusion mechanism as a mechanism of material removal, however, is not conclusive. Other mechanisms of material removal undoubtedly occur, but one must necessarily rely on the assumption that one or two of these mechanisms control if analytic work is to be done.

Clearly, some critical experiments are required to clarify this matter. The first suggestion is that attention should be concentrated on the more macroscopic mechanism of material removal as opposed to a microscopic investigation. The latter method of pursuit is obviously a part in the logical sequence to determine and verify the physical mechanisms controlling behavior, but a knowledge of microscopic behavior is difficult to apply if there is no information to bridge the gap between it and general mechanical behavior. With this in mind it seems best to investigate the assumptions on which the proposed mechanism is based.

Material is assumed to spread as a result of a harder subsurface, which may be due to either work hardening or the embedment of abrasive particle fragments. The behavior of protrusions subjected to angular particles impinging at a near-normal angle could then be studied in three separate cases:

1. A protrusion is created in an unhardened material without altering the pre-existing stress-strain distribution around it; say be chemical etching or some form of machining followed by an anneal.
2. The protrusion is created by mechanically depressing material all around it.
3. Particle fragments are somehow mixed in the material, and a protrusion subsequently made.

Experiments of this form would give more information as to whether the proposed mechanism governs and why.

Eventually, it would be ideal if this process could be modeled analytically as a further test to its applicability.

ACKNOWLEDGMENTS

I am indebted to Prof. Iain Finnie for his guidance and inspirations throughout the course of this project. Mr. Alan V. Levy, Director of the Erosion/Corrosion Program, also offered some helpful suggestions. I would like to thank the entire staff of the Materials and Molecular Research Division of Lawrence Berkeley Laboratory without whom my experimentation would not have been possible. My appreciation is also extended to Professor F. Hauser and Professor V. Zackey who reviewed this thesis.

The work, conducted at the Materials and Molecular Research Division of Lawrence Berkeley Laboratory, was supported by the Basic Energy Sciences Division of the Department of Energy.

REFERENCES

1. D. H. McFadden, "Erosion of Ductile Metals by Solid Particles," Lawrence Berkeley Laboratory Report LBL-6279 (1977).
2. A. W. Ruff and L. K. Ives, "Measurement of Solid Particle Velocity in Erosive Wear", Wear 35, 195 (1977).
3. R. E. Winter and I. M. Hutchings, "Solid Particle Erosion Studies Using Single Angular Particles," Wear, 29, 181-194 (1974).
4. G. L. Sheldon and I. Finnie, "On the Ductile Behavior of Nominally Brittle Materials During Erosive Cutting", J. Eng. Ind., 88, 4, 387-392 (1966).
5. I. Finnie, "An Experimental Study of Erosion", Proc. Soc. Exp. Stress Anal., 18, 2, 65-70 (1960).
6. C. E. Smeltzer, M. E. Gulden, and W. A. Compton, "Mechanisms of Material Removal by Impacting Dust Particles", J. Basic Eng., Trans. ASME, 639-654 (Sept. 1970).
7. G. P. Tilly, "A Two-Stage Mechanism of Ductile Erosion," Wear, 23, 87-96 (1973).
8. I. Finnie, "Some Observations on the Erosion of Ductile Metals", Wear, 19, 81-90 (1972).
9. G. L. Sheldon, "Effects of Surface Hardness and other Material Properties on Erosion Wear of Metals by Solid Particles," J. Eng. Mater. Technol., 9, Ser. H, No. 2, 133-137 (1977).
10. L. L. Brass, "The Effects of Microstructure of Ductile Alloys on Solid Particle Erosion", Lawrence Berkeley Laboratory Report LBL-6277 (1977).

11. I. Finnie, "The Mechanism of Erosion of Ductile Metals", ASME Proc. Third U.S. Natl. Congress Appl. Mech., 527-532 (1958).
12. I. Finnie and D. H. McFadden, "On the Velocity Dependence of the Erosion of Ductile Metals by Solid Particles at Low Angles of Incidence" (to be published in Wear).
13. T. O. Mulhearn and L. E. Samuels, "Abrasion of Metals - Model of Process", Wear, 5, 478-498 (1962).
14. J. G. A. Bitter, "A Study of Erosion Phenomena: Part 1", Wear, 6, 5-21 (1963).
15. P. Ascarelli, "Relation Between the Erosion by Solid Particles and the Physical Properties of Metals," AMMRC, TR 71-47 (Nov. 1971).
16. N. P. Suh, "The Delamination Theory of Wear", Wear, 25, 111-124 (1973).
17. J. M. Hutchings, and R. E. Winter, "Particle Erosion of Ductile Metals: A Mechanism of Material Removal", Wear, 27, 121-128 (1974).
18. G. L. Sheldon and A. Kanhere, "An Investigation of Impingement Erosion Using Single Particles", Wear, 21, 195-209 (1972).
19. I. Kleis and H. Uemois, "Untersuchung des Strahlverschleiss Mechanisms von Metallen" (Investigation of the Mechanisms of Abrasive Stream Wear of Metals), J. Mater. Technol. 5, Nr. 7, 381-389 (1974).

This report was done with support from the Department of Energy. Any conclusions or opinions expressed in this report represent solely those of the author(s) and not necessarily those of The Regents of the University of California, the Lawrence Berkeley Laboratory or the Department of Energy.

